*Article*

# Study of the Mobilization of Uranium Isotopes in a Sandstone Aquifer Using Methods for the Extraction of Uranium with Different Strength Reagents in Combination with Groundwater Data

**Alexander I. Malov*** and **Sergey B. Zykov**

Federal Center for Integrated Arctic Research of Russian Academy of Sciences; Arkhangelsk, 163061, Russia; malovai@yandex.ru; abs2417@yandex.ru

* Correspondence: malovai@yandex.ru; Tel.: +7-911-571-71-72

**Abstract:** A partial extraction procedure was used to study the distribution of uranium in the mineral phases of rocks of an aquifer of sandy-clay deposits of the Vendian in the northwest of Russia. This work is a part of a research project to develop a method for combined radiocarbon and uranium-isotope dating of groundwater. Representative aliquots of each core sample were subjected to five "partial" extractions by treatment with: distilled water, low mineralized fresh natural groundwater, minopolycarboxylic acid chelating agent (0.05M EDTA), 0.5M HCl, 15M $HNO_3$, and a total digestion, with U isotopes reported in this study for each procedure. The following mineral phases of core samples: adsorbed material, carbonate minerals, amorphous iron oxides, aluminosilicates partial digestion and a crystalline iron oxides, aluminosilicates total digestion and a clay/quartz resistate were characterized. Red-colored siltstones depleted in uranium in relatively readily soluble mineral phases. The concentration of adsorbed uranium was established in the amount of 15.8±2.1 - 30.5±3.9 µg/kg. Carbonate minerals contain even less of this element. In iron hydroxides and the most readily soluble aluminosilicates, its concentrations are in the range 168±24 - 212±28 µg/kg. The most insoluble fraction contains 1.65±0.21 - 4.32±0.45 mg/kg of uranium. In green-colored siltstones, the concentration of adsorbed uranium is much higher: 106±14 - 364±43 µg/kg. Carbonate minerals and amorphous iron oxides contain 1.91±0.21 - 2.34±0.26 mg/kg of uranium. In aluminosilicates and a clay/quartz resistate, uranium concentrations are 5.6±0.5 - 16.8±1.4 mg/kg. Elevated values of $^{234}U{:}^{238}U$ activity ratio prevail in the adsorbed material and iron hydroxides. In aluminosilicates and clay/quartz resistate, the values decrease. This indicates the replacement of primary sedimentogenic uranium by secondary hydrogenic uranium adsorbed on the surface of minerals and coprecipitated with iron hydroxides. The results obtained made it possible to carry out preliminary quantitative estimates of the retardation factor and recoil loss factor of uranium in the groundwater of siltstones of the studied Vendian aquifer.

**Keywords:** Partial extraction, Mineral phases, Uranium, Disequilibrium, Retardation factor

## 1. Introduction

Uranium isotopes are a powerful tool for refining conceptual models of groundwater [1–4], groundwater dating [5–7] and descriptions of chemical weathering processes [8–10] for up to hundreds of thousands of years [11]. The main initial parameters are i) measured concentration of $^{238}U$ in the combined solution and solid phase, and ii) measured $^{234}U{:}^{238}U$ activity ratio in the

40  combined pore fluid and solid phase. They can be obtained by direct measurements in water and
41  rock samples taken in the field.

42      However, the interpretation of the results is rather complicated. This is due to the heterogeneity
43  of the rocks in their composition. For example, sandy clay sediments of aquifers can contain both
44  poorly soluble grains of quartz and feldspar, as well as soluble carbonate and gypsum cements.
45  Carbonates, iron oxides, and clay minerals are characterized by increased U adsorption on their
46  surfaces [12–14]. Further, daughter nuclides pass most actively into water from surface coatings [15],
47  increasing the ratio of isotope activities in water. In addition, the similarity of the activity ratios of
48  $^{234}$U:$^{238}$U in groundwater and in the most easily leached fractions of water-bearing rocks was noted in
49  the experiments of Lowson et al. [16] , Payne et al. [17], and Dabous et al. [18]. These fractions were
50  defined as adsorbed elements, carbonate minerals and amorphous iron minerals [19]. This may
51  indicate the opposite process: the transition of nonequilibrium nuclides from water to rock with an
52  increase in the ratio of U isotope activities in the rock [20]. Under such conditions, it is difficult to
53  estimate the rate of chemical weathering by using the currently developed methods [21-22].

54      Therefore, for a more complete understanding of the behavior of uranium isotopes in the
55  water-rock system, a transition from the presentation of solely total concentration and activity data
56  to an additional analysis for finding individual "weak" leach extractants or sequential extractions is
57  necessary. In recent decades, leach data, rather than total decomposition data are widely used in a
58  variety of fields of geoecology (see for example [23-26]). Therefore, in the present work, an attempt is
59  made to use the partial extraction procedure for reconstructing the processes of redistribution of
60  uranium isotopes in certain mineral phases of an aquifer of sandy-clay deposits of the Vendian.

61      In a previous papers [27-28], the possibility of sharing uranium and carbon isotopes for dating
62  groundwater was discussed. The transport of uranium in solution is reasonably well described with
63  a standard advection-dispersion-exchange formulation:

64  $\Delta time = advection + weathering + recoil + desorption + production - precipitation - decay - adsorption$
65  [5-7]. Among the many factors, the main ones are $t$ – Groundwater residence time in the aquifer
66  (time), $v$ – Groundwater flow velocity (advection), $R_d$ – Dissolution rate (weathering - precipitation),
67  $R$ – Retardation factor (adsorption - desorption), $p$ – Recoil loss factor (recoil + production), and $\lambda_4$ –
68  Decay constants for $^{234}$U (decay). Suitable equations were derived by Andrews and Kay [29],
69  Fröhlich and Gellermann [30], Ivanovich et al. [9], and Porcelli [5] to provide a $^{234}$U–$^{238}$U dating
70  method for groundwater under oxidizing conditions. However, the values of $R$, $R_d$ (a$^{-1}$) and $p$ needed
71  to be determined. In turn, the recoil loss factor value $p$ depends on the *SSA* (specific surface area).
72  The published *SSA* values in sandy aquifers range from 0.9–1.8 m$^2$.kg$^{-1}$ [31] to 330–390 m$^2$.kg$^{-1}$ [6].
73  Accordingly, the ranges of $R$ and $R_d$ can be calculated using these formulas. Therefore, we consider it
74  more appropriate to show $R$, $R_d$ and $p$ in the form of their ratios: $R_d$:$p$ (a$^{-1}$), $R$:$p$ and $R_d$:$R$ (a$^{-1}$) . The
75  main calculated equations are as follows [27]:

76
$$t = \frac{\ln(k^{-1})}{\lambda_4} \text{ , where } k = 1 - \frac{C_8{}^W \cdot R \cdot (AR_t - 1)}{M_s \cdot C_8{}^R \cdot p} \tag{1}$$

77    Where $C_8{}^W$ is the concentration of uranium in water; $C_8{}^R$ is the concentration of uranium in

78    the rock; $AR_t$ - $^{234}$U/$^{238}$U is the activity ratio in the water sample; $M_s$ is the solid mass to fluid

79    volume ratio.

80    In this case, two unknown parameters remain in formula (1), which cannot be directly

81    measured in water and rock samples: $t$ and $R/p$. Therefore, in order to use equation (1), it is

82    necessary to make several determinations of the groundwater age by other methods, for example,

83    using isotopes of carbon. Then, we need to find out whether there is an increase in uranium

84    concentrations in groundwater with a decrease in the concentration of radiocarbon. If this is the case,

85    then the mean values $R/p$ for the studied aquifers are determined. After this, uranium-isotopic

86    dating of other groundwater samples is carried out, which is less labor-intensive and more accessible

87    than radiocarbon dating. The average value of the retardation factor/recoil loss factor ratio ($R/p$) in

88    samples from the sandstone aquifer of the upper Vendian strata and overlying horizons is assumed

89    to be (24±4) [27].

90    In this work, it was planned, by determining the amount of uranium adsorbed on the surface of

91    mineral particles, to proceed to a separate assessment of the values of the retardation factor and

92    recoil loss factor of uranium in the groundwater of siltstones of the studied Vendian aquifer.

93    **2.    Materials**

94    The borehole GGS2-11 is located in the northwest of Russia at the diamond deposit area

95    (N65°20'48" E41°06'10") and was drilled using a diamond drill bit (92 mm inner diameter, 112 mm

96    outer diameter) and mud rotary methods to 101.2 m below ground surface in July 2018. This core

97    was selected for the present study because the sampled section traverses the aquifer of the Padun

98    formation of the Vendian (Vpd) [27, 28] which is of interest in the present study. For this study, 5

99    samples were taken from the intervals of 66.7-66.8, 75.2-75.3, 83.9-84, 94-94.1, 99.5-99.6 m (Fig. 1).

100    The samples were quickly packed in airtight polythene bags. The sample mass collected in each

101    case was about 1500 g. Sub-samples of the material were oven dried at 40 °C for 7 days and

102    homogenized by grinding with an agate mortar and pestle to pass through a 125 μm sieve. The

103    prepared material was stored in glass bottles for sequential extractions and isotopic analyses.

104    The chemical and mineralogical composition of the Vendian deposits in the area of the diamond

105    deposit was studied in detail during different periods of geological exploration [32-35]. The Padun

106    Formation, 160 m thick, mainly consists of sandstones (60-80%) and siltstones (20-30%) separated by

107    mudstone interlayers. The rocks have reddish brown color with pale green lenses and patches. The

108    sandstones are dominated by fine- and medium-grained varieties. The content of pelitic particles

109    does not exceed 20%. Clastic material is represented by quartz. Feldspars, chalcedony, quartzite

110    fragments, biotite, and clayey aggregates are insignificant. The cement has mainly a clayey

111    (hydromicaceous)-ferruginous composition. Carbonate and gypsum cement is also encountered. In

112    the upper part of the sequence (thickness ~50 m), the sandstones are poorly cemented and often

113    represented by sands. The siltstones are dominated by the coarse-grained fraction. The clastic grains

114    consist of quartz (up to 98%), feldspars (up to 10%), and micas (~1%). The cement has

115    clayey-ferruginous, carbonate-clayey, and less common gypsum compositions. Clay minerals are

116    observed as hydromicas, kaolinite, and chlorite. Bitumen and organic carbon are nearly absent. The

117    ratio of $Fe_2O_3$ and FeO forms of iron in "red" siltstones is ~ 17: 1. In "green" siltstones, the $Fe_2O_3$
118    content is 2.7 times lower (Table 1).

119



120

**Figure 1.** Photos of samples of studied rocks. 1 - Green siltstones, 66.7-66.8 m. 2 - Red sandstones, 75.2-75.3 m. 3 - Variegated siltstones, 83.9-84 m. 4 - Red siltstones, 94-94.1 m. 5-6 - Green siltstones, 99.5-99.6 m (photo S. Druzhinin)

124    The description of the samples of the studied rocks was performed on five thin sections of core
125    samples (see Appendix A).

126    **Table 1.** The average chemical composition of the red siltstones of the Padun Formation of the
127    Vendian in research area (from 18 determinations) [34] and green siltstones of the sample GGS2-11
128    (depth 99.5 m), %

|  | $SiO_2$ | $Al_2O_3$ | CaO | MgO | $Na_2O$ | $K_2O$ |
|---|---|---|---|---|---|---|
| [a] RSi | 72 | 12.8 | 0.48 | 1.24 | 0.14 | 2.94 |
| [b] GSi | 74.6 | 12.5 | 0.39 | 1.34 | 0.16 | 4.48 |

129

|  | $Fe_2O_3$ | FeO | $TiO_2$ | $Cr_2O_3$ | MnO | $P_2O_5$ | [c] LOI |
|---|---|---|---|---|---|---|---|
| [a] RSi | 5.3 | 0.3 | 0.81 | 0.02 | 0.14 | 0.07 | 3.36 |
| [b] GSi | 1.99 | 0.3 | 0.91 | 0.07 | 0.01 | 0.11 | 2.74 |

130    [a] RSi - red siltstones. [b] GSi - green siltstones. [c] LOI - loss on ignition.

131    **3.    Methods**

132    Representative aliquots of each core sample were subjected to five "partial" extractions and a
133    total digestion, with U isotopes reported in this study for each procedure. The various procedures
134    are described hereinafter.

135  3.1.   Partial extractions
136       *Distilled water*
137       500 ml distilled water was mixed with 50 g of core sample in centrifuge tubes and shaken for 1
138  hr on an end-over-end shaker at room temperature. The short duration of the laboratory
139  experiments suggests that dissolution depends upon the ease with which the fine particulates may
140  be freed from the rock surface [36-37]. Firstly, this procedure refers to adsorbed particles.
141       *Low mineralized fresh natural groundwater*
142       500 ml of low mineralized water of Ca-Mg-Na-$HCO_3$ composition from the borehole had total
143  dissolved solids (TDS) of 285 mg/L (see [28]) and was mixed with 50 g of core sample in centrifuge
144  tubes and shaken for 1 hr on an end-over-end shaker at room temperature. Firstly, adsorbed
145  material was released.
146       The following four stages were carried out according to the method proposed by Sutherland et
147  al. [26].
148       *0.05M EDTA*
149       Aminopolycarboxylic acid chelating agent (EDTA) at the concentration and pH level used in
150  this study was the weakest extractant after fresh groundwater [26]. As an extractant, EDTA has
151  been widely used in environmental geochemistry. Complexants like EDTA are frequently used to
152  release the readily available (labile) fraction of materials [26]. In our case, this is carbonate cement.
153  The procedure outlined by Singh et al. [38] was followed in this study. 500 mL of 0.05M EDTA (pH
154  7) was mixed with 50 g of core sample in centrifuge tubes and shaken for 1 hr on an end-over-end
155  shaker at room temperature.
156       *0.5M HCl*
157       According to a review by Sutherland et al. [26], HCl dissolves complexed, adsorbed,
158  precipitated, amorphous or poorly crystallized Fe compounds without significant attack on the
159  crystal lattice. In the present study, 500 mL of 0.5M HCl was mixed with 50 g of core sample and
160  shaken at room temperature for 1 hr on an end-over-end shaker.
161       *15M $HNO_3$*
162       Nitric acid is an oxidizing agent that is not as powerful in its attack on aluminosilicates as HF,
163  and is thus said to be a partial digestion. Also, crystalline iron oxide is digested by hot $HNO_3$. In the
164  present study, 500 mL of 15M $HNO_3$ was mixed with 25 g of core sample and heated for 1 hr while
165  stirring. The resulting solution was evaporated to wet salts, topped up with 500 ml of distilled water
166  and acidified with HCl to pH 1-2.
167  3.2.   Measurements of uranium isotopes after five "partial" extractions
168       Determinations of uranium isotopes in the resulting solution were made in accordance with
169  Malyshev et al. [39] which is also described in Fröhlich [40]. Spectrometric detection of alpha
170  particles was performed using an alpha spectrometer (PROGRESS-ALPHA, 'DOZE', Russia) with
171  uncertainty of 10-15%. Total error of analysis is defined by $\delta = \delta_{st} + \delta_{sys}$ (statistical + systematic).
172  Measurement uncertainties for U are reported individually (Table 2). Efficiency of $^{232}U$ extraction
173  was 40-50%.
174  3.3.  Total digestion
175       Measurements of uranium isotopes were made in accordance with Malyshev et al. [41]. For
176  these analyses, 10 g of core sample was placed in a porcelain crucible and calcined at 500 °C until
177  complete combustion of organic substances. The residue was transferred into a Teflon cup wetted
178  with distilled water. A weighed amount of spiked solution (with known activity of internal
179  standard $^{232}U$) was added, followed by 10 $cm^3$ of 15M $HNO_3$ and then heated until the reddish
180  brown $NO_2$ gas vapor disappears. Then after cooling 40 $cm^3$ of 29M HF and 10 $cm^3$ of 12M $HClO_4$
181  were added. The covered Teflon cup was heated until $HClO_4$ vapor appeared. HF treatment was
182  repeated twice; the cup was cooled each time before adding acid and heating until $HClO_4$ fumes
183  were visible. After dissolution and cooling, the edge of the cup and the cover were rinsed with
184  distilled water and the content was transferred to an open Teflon™ dish, where the solution was
185  evaporated again until dense white fumes appeared. This procedure was repeated twice. Finally,
186  the residue was evaporated to give moist salts, which were dissolved in boiling 7M $HNO_3$ (50 $cm^3$).
187  The undissolved residue was filtered off and washed three times with 5-10 $cm^3$ portions of hot 7M
188  $HNO_3$ and added to the solution. The U solution was transferred to a separatory funnel and a 30%

189  solution of freshly purified tributylphosphate in toluene was added to give an aqueous to organic
190  phase ratio of 4:1. Radionuclides were extracted for 5 min. After phase separation, the lower layer
191  was poured back into the beaker. The organic extract was washed twice with an equal volume of
192  7M $HNO_3$, then with an equal volume of 0.25M $HNO_3$ solution in 0.04M HF. The back-extraction of
193  uranium isotopes was performed by washing the organic phase with an equal volume of distilled
194  water three times for 1 min each. The pooled aqueous extracts were evaporated to dryness, treated
195  with 5 $cm^3$ of concentrated $HNO_3$ to remove trace organic substances, and evaporated to dryness.
196  The dry residue containing uranium was dissolved in 10 mL of 2% sodium carbonate with heating,
197  then filtered. Dissolved uranium was electrodeposited on polished stainless steel plates for alpha
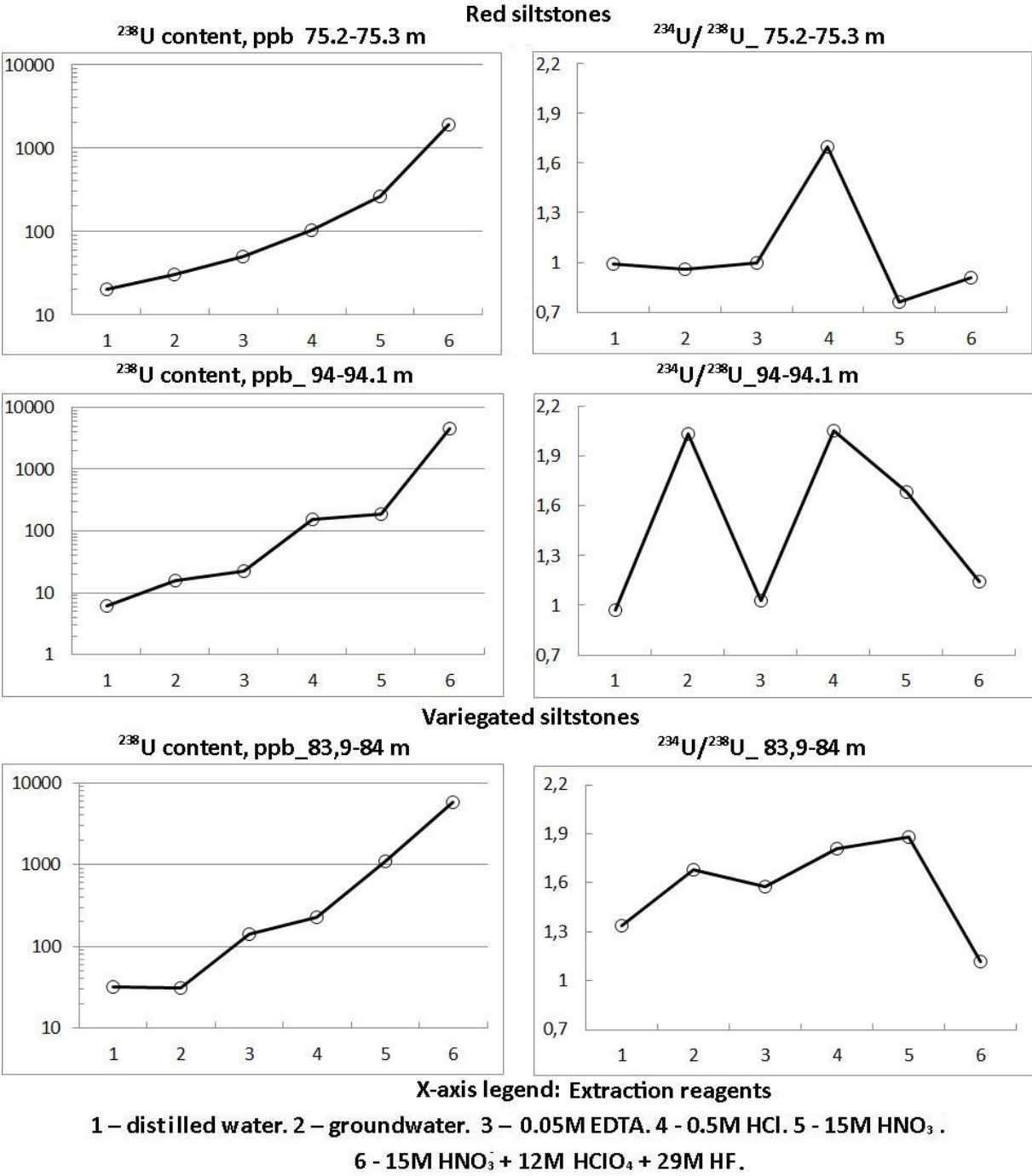198  spectrometry.
199
200  **4.    Results**

201        Table 2 and Figs. 2 and 3 show the results of five "partial" extractions and total digestion of the
202  five core samples.
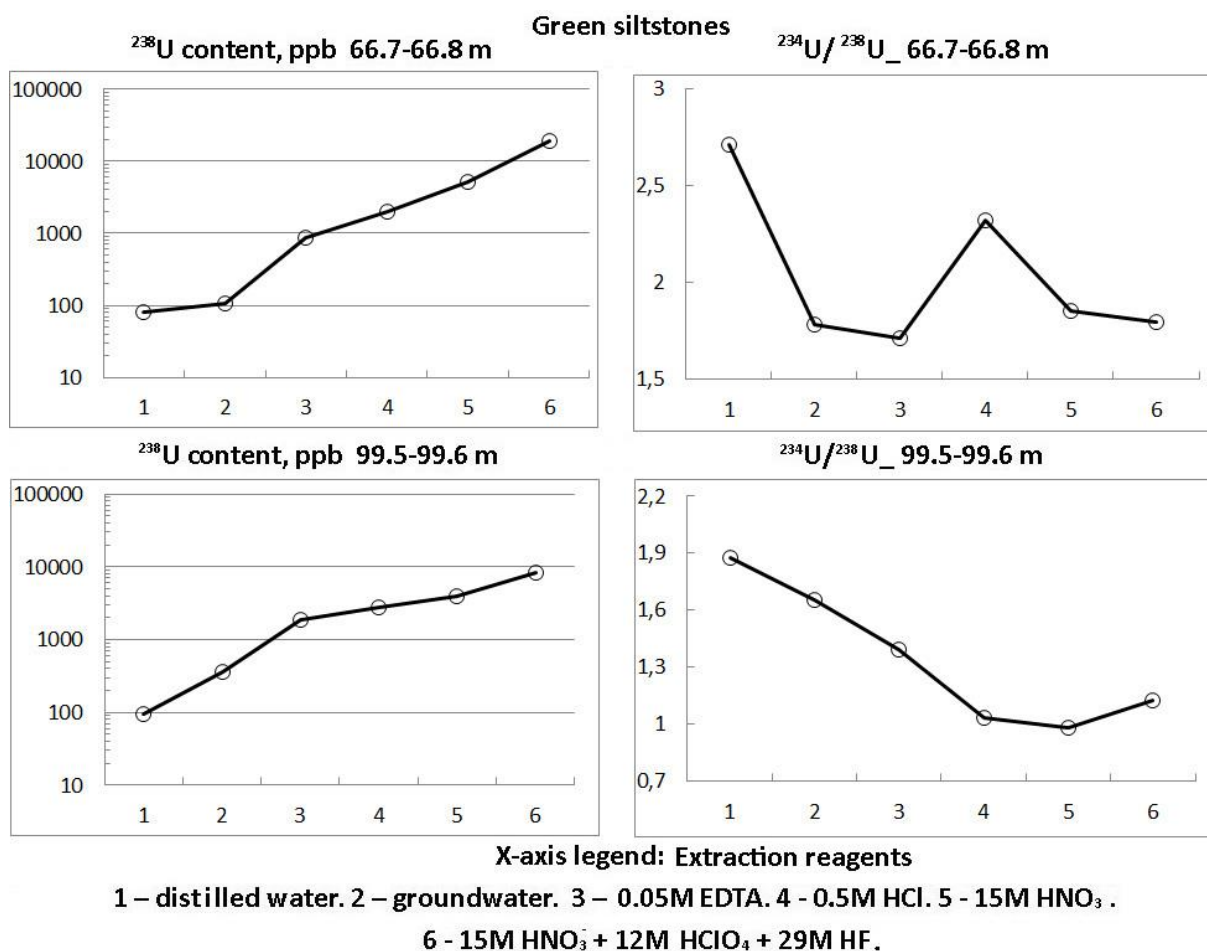
203        **Table 2.** Distribution of uranium and measured $^{234}U$:$^{238}U$ activity ratios in extracted phases

| Solvent | [a] DW | [b] GW | 0.05M EDTA | 0.5M HCl | 15M $HNO_3$ | 15M $HNO_3$ + 12M $HClO_4$ + 29M HF |
|---|---|---|---|---|---|---|
| **Substance dissolution, %** | | | | | | |
| Red siltstones | 0.49 – 0.6 | 0.62 - 1 | 2.4 – 3.4 | 1.58 - 2.27 | 1.82 - 3.42 | 100 |
| Variegated siltstones | 1.04 | 0.82 | 1.88 | 2.3 | 4.34 | 100 |
| Green siltstones | 0.93 - 1.38 | 0.64 - 1.93 | 0.94 - 3.08 | 2.56 - 6.34 | 6.85 – 15.4 | 100 |
| Average | 0.89 | 1 | 2.34 | 3.01 | 6.37 | 100 |
| **U content, µg/kg** | | | | | | |
| Red siltstones 1 | 6.2±0.9 | 15.8±2.1 | 22.8±3.2 | 156±23 | 191±27 | 4510±467 |
| Red siltstones 2 | 20±2.6 | 30.5±3.9 | 50.3±7.4 | 103±14 | 262±34 | 1910±243 |
| Variegated siltstones | 31.6±4.6 | 30.9±4.1 | 140±19 | 230±28 | 1102±143 | 5840±578 |
| Green siltstones 1 | 80±11.1 | 106±14 | 857±102 | 2014±215 | 5086±512 | 18800±1504 |
| Green siltstones 2 | 95.3±11.4 | 364±43 | 1860±203 | 2708±302 | 3957±415 | 8328±707 |
| Average | 46.6 | 109 | 586 | 1042 | 2120 | 7878 |
| **U content, %** | | | | | | |
| Red siltstones | 0.14 - 1.1 | 0.35 - 1.6 | 0.51 - 2.6 | 3.5 - 5.4 | 4.2 - 13.7 | 100 |
| Variegated siltstones | 0.54 | 0.53 | 2.4 | 3.94 | 18.9 | 100 |
| Green siltstones | 0.43 - 1.14 | 0.56 - 4.37 | 4.56 - 22.3 | 10.7 - 32.5 | 27.1 - 47.5 | 100 |
| Average | 0.67 | 1.48 | 6.47 | 11.2 | 22.3 | 100 |
| **$^{234}U$:$^{238}U$ activity ratio** | | | | | | |
| Red siltstones | 0.97±0.14 - 0.99±0.14 | 0.96±0.13 - 2.3±0.32 | 1±0.14 - 1.03±0.14 | 1.7±0.25 - 2.05±0.29 | 0.76±0.11 - 1.68±0.22 | 0.91±0.13 - 1.14±0.16 |
| Variegated siltstones | 1.34±0.19 | 1.68±0.23 | 1.58±0.21 | 1.81± 0.24 | 1.88±0.24 | 1.12±0.14 |
| Green siltstones | 1.87±0.26 - 2.71±0.36 | 1.65±0.2 - 1.78±0.24 | 1.39±0.2 - 1.71±0.24 | 1.03±0.15 - 2.32±0.33 | 0.98±0.14 - 1.85±0.25 | 1.12±0.14 - 1.79±0.24 |
| Average | 1.58 | 1.67 | 1.34 | 1.78 | 1.43 | 1.22 |

204  [a] DW - Distilled water. [b] GW – groundwater.

**Figure 2.** Distribution of $^{238}U$ content and $^{234}U$:$^{238}U$ activity ratio in phases 1-6, leached from crushed red and variegated siltstone of Vendian (Ediacaran) Padun Formations

**Figure 3.** Distribution of $^{238}$U content and $^{234}$U:$^{238}$U activity ratio in phases 1-6, leached from crushed green siltstone of Vendian (Ediacaran) Padun Formations

*Substance dissolution*

As can be seen from Table 2, water dissolved on average about 1% of the samples of siltstones. At the same time, green siltstones dissolved approximately two-fold more intensively. The following solvents, EDTA and 0.5M HCl, are further dissolved in approximately 1% of each. The ratio of red and green siltstones dissolved in hydrochloric acid remains ~ 1:2. The impact of EDTA on both types of rocks is approximately the same. Nitric acid additionally dissolves an average of 3.36% of the rock. Green siltstone dissolves with nitric acid 2.5-fold more intensively than with hydrochloric acid. The bulk of the rock, from 96.58 to 98.18% red siltstones and from 84.6 to 93.15% green siltstones, is dissolved only with a mixture of 15M $HNO_3$ + 12M $HClO_4$ + 29M HF acids.

*Uranium concentration*

In red siltstones, the total uranium content was 1910±243 - 4510±467 µg/kg. The material dissolved in groundwater contained 15.8±2.1 - 30.5±3.9 µg/kg. Three subsequent solvents bring the uranium content in the material dissolved by them to 191±27 - 262±34 µg/kg, which is only 4.2 - 13.7% of the total uranium content in red siltstones. The main supply of uranium is contained in these rocks in the highest degree of barely soluble fraction, extractable by complete digestion.

In green siltstones, the total uranium content was 8328±707 - 18800±1504 µg/kg. The material dissolved in groundwater contained 106±14 - 364±43 µg/kg. Three subsequent solvents brought the uranium content in the material dissolved by them to 3957±415 - 5086±512 µg/kg, which is already 27.1 - 47.5% of the total uranium content in green siltstones. The most insoluble fraction, respectively, contained 52.5 - 72.9% of uranium.

*$^{234}$U:$^{238}$U activity ratio*

In red siltstones, the maximum values of $^{234}$U:$^{238}$U activity ratio (1.7±0.25 – 2.3±0.32) were noted in the material dissolved in groundwater and 0.5M HCl. Minimum values (0.76±0.11 – 0.91±0.13) are

235 characteristic of the most difficultly soluble 15M $HNO_3$ and 15M $HNO_3$ + 12M $HClO_4$ + 29M HF
236 fractions of the studied rocks. In other cases, the values are close to unity.
237      In green siltstones, one increased value of $^{234}U$:$^{238}U$ activity ratio (2.32±0.33) was noted in a
238 material dissolved in 0.5M HCl. Three values close to unity were obtained by dissolving 0.5M HCl,
239 15M $HNO_3$ and 15M $HNO_3$ + 12M $HClO_4$ + 29M HF. However, in the remaining eight experiments,
240 using groundwater, 0.05M EDTA, 15M $HNO_3$, and 15M $HNO_3$ + 12M $HClO_4$ + 29M HF as a solvent,
241 the values of $^{234}U$:$^{238}U$ activity ratio were high: 1.39±0.2 – 2.71±0.36.

242 **5.    Discussion**

243      *Substance dissolution*
244      In general, the percentage values of the substance dissolved under the influence of various solvents are
245 approximately consistent with the average chemical composition of siltstones of the Padun Formation of the
246 Vendian in the study area. EDTA, the weakest extractant after fresh groundwater, dissolved up to 3.4% of the
247 substance (Table 2). This corresponds to a loss on ignition (LOI) of 2.74 - 3.36% (Table 1), i.e. the carbonate
248 material of the cement of the studied rocks and other labile fractions. 0.5M HCl additionally dissolved up to 3%
249 of the substance, which is consistent with the content of $Fe_2O_3$ (2 - 5.3%) in Table 1, that is, it corresponds to
250 amorphous iron oxides. 15M $HNO_3$ additionally dissolved up to 9% of a substance that can only be represented
251 by the most readily soluble aluminosilicates. A mixture of 15M $HNO_3$ + 12M $HClO_4$ + 29M HF acids dissolves
252 the remainder of the aluminosilicates and a clay/quartz resistate.
253      *Uranium concentration*
254      Table 3 shows the uranium concentrations converted to mineral phases in μg/kg and %. In red siltstones,
255 the concentrations of adsorbed uranium were established in the amount of 15.8±2.1 - 30.5±3.9 μg/kg. This
256 amounts to 0.35 - 1.6% of its total amount in rocks of this type. Carbonate minerals contain even less uranium:
257 7±1 – 19.8±2.5 μg/kg. In iron hydroxides and the most readily soluble aluminosilicates, uranium concentrations
258 are in the range 52.7±7.2 - 133±19 and 35±5 - 159±21 μg/kg, respectively. This amounts to a total of 3.7 - 11.1%
259 of its total concentration. The most insoluble fraction contains 1.6±0.2 – 4.3±0.4 mg/kg of uranium. In green
260 siltstones, the concentration of adsorbed uranium is much higher: 106±14 - 364±43 μg/kg (0.56 - 4.37%). The
261 carbonate minerals and amorphous iron oxides contain a total of 1.91±0.21 – 2.34±0.26 mg/kg of uranium
262 (10.15 – 28.2%). In aluminosilicates and a clay/quartz resistate, the concentration of uranium amounts to
263 5.6±0.5 – 16.8±1.4 mg/kg.

264      **Table 3.** Distribution of uranium in the mineral phases.

| Defined phases of core samples | Adsorbed elements | Carbonate minerals | Amorphous iron oxides | Aluminosilicates partial digestion and a crystalline iron oxides | Aluminosilicates total digestion and a clay/quartz resistate |
|---|---|---|---|---|---|
| **U content, μg/kg** | | | | | |
| Red siltstones 1 | 15.8±2.1 | 7±1 | 133±19 | 35±5 | 4319±447 |
| Red siltstones 2 | 30.5±3.9 | 19.8±2.5 | 52.7±7.2 | 159±21 | 1648±210 |
| Variegated siltstones | 30.9±4.1 | 109±15 | 90±11 | 873±113 | 4738±469 |
| Green siltstones 1 | 106±14 | 751±89 | 1157±123 | 3072±309 | 13714±1097 |
| Green siltstones 2 | 364±43 | 1496±163 | 848±95 | 1249±131 | 4371±371 |
| **U content, %** | | | | | |
| Red siltstones 1 | 0.35 | 0.16 | 3 | 0.7 | 95.8 |
| Red siltstones 2 | 1.6 | 1 | 2.8 | 8.3 | 86.3 |
| Variegated siltstones | 0.53 | 1.87 | 1.54 | 14.96 | 81.1 |
| Green siltstones 1 | 0.56 | 4 | 6.15 | 16.3 | 72.9 |
| Green siltstones 2 | 4.37 | 18 | 10.2 | 15 | 52.5 |

265

266      *$^{234}U$:$^{238}U$ activity ratio*

267    Increased values of $^{234}$U:$^{238}$U activity ratio were noted in the material of red siltstones dissolved
268    in water and 0.5M HCl. That is, uranium isotopes with elevated values of $^{234}$U:$^{238}$U activity ratio
269    (greater than 1) were deposited from groundwater on sorbent material and with iron hydroxides.
270    Reduced values of $^{234}$U:$^{238}$U activity ratio (less than 1) are characteristic of the most difficultly soluble
271    fractions. In them, the dissolution of uranium by groundwater was practically absent and only
272    depletion of $^{234}$U atoms occurred due to recoil loss factor. In green siltstones, there is also a tendency
273    towards a decrease in $^{234}$U:$^{238}$U activity ratio in the direction from easily soluble fractions to sparingly
274    soluble fractions (Fig. 3, interval 99.5–99.6 m). However, for a sample taken from the interval 66.7 -
275    66.8 m, high values of $^{234}$U:$^{238}$U activity ratio are observed in all mineral phases. Additional studies
276    are needed to explain this fact.
277    *Evolution of uranium isotopic compositions*
278    The results obtained partially confirm previously expressed ideas about the evolution of U
279    isotopic compositions of the Vendian rock near the study area [20]. It has been established that the
280    processes of chemical weathering of Vendian deposits led to the formation of a strong oxidation
281    zone, developed above 250 m.b.s.l. The inverse correlation between the concentrations of U and Fe
282    (see Tables 1 and 2) in the red siltstones (increased Fe concentrations and reduced U contents) is a
283    result of removal of U in oxidizing conditions, and accumulation of Fe. In red siltstones, the
284    concentration of Fe$_2$O$_3$ is 5.3%, and the content of U is 1.9-4.5 mg/kg, in green siltstones the
285    concentration of Fe$_2$O$_3$ is 2%, and the content of U is 5.8-18.8 mg/kg. Almost all U in the red siltstones
286    has been replaced by a newly formed "hydrogenic" U (precipitated from groundwater), with an
287    initial $^{234}$U:$^{238}$U activity ratio ≈ activity ratio of modern fresh groundwater = 3. The ending of the
288    period of co-precipitation of hydrogenic uranium with iron hydroxide was estimated as 0.9 Ma,
289    which should roughly correspond to the period of a sharp cold snap in the region. After, dissolution
290    and desorption of hydrogenic U occurred during periods with no glaciations and marine
291    transgressions.
292    Our results are consistent with the experimental results of Lowson et al. [16], Payne et al. [17],
293    and Dabous et al. [18], which note the similarity of the $^{234}$U:$^{238}$U activity ratios in groundwater and in
294    the most easily leached fractions of water-bearing rocks.
295    At the same time, the lower average value of $^{234}$U:$^{238}$U activity ratio 0.92 [20] was established in
296    the samples of green siltstones taken in the paleovalley, which was screened by the layer of sea clays.
297    It is explainable by the fact that these deposits have reached a steady state of the $^{234}$U:$^{238}$U activity
298    ratio that depends only on their size (the average grain size ≈ 30 μm), because they were under
299    reducing conditions over 1 Ma. A significantly higher content of uranium in them compared to red
300    siltstones shows a considerable variability in the permeability values of the aquifer, whereby they
301    were away from the paths of groundwater filtration and have retained uranium. The green siltstones
302    studied in this work occur in the oxidative conditions of the aquifer which contains young fresh
303    water [28]. They have high concentrations of uranium in readily soluble fractions and high $^{234}$U:$^{238}$U
304    activity ratios. This can be explained by their deep processing by groundwater in a relatively recent
305    period (tens - the first hundreds of thousands of years). During this processing, they were in a loose
306    state, as a result of which U was evenly precipitated from water on the surface of disintegrated rock
307    particles in the entire volume of the current green siltstones. Then there was cementation of rocks
308    with Fe hydroxides, carbonates and clay material. After this, the rocks were again compacted under
309    glacial loading. As the second option, it can be assumed that the green siltstones replace lenticular
310    accumulations of organic matter with a high content of U adsorbed from groundwater. The place
311    where 5 samples were taken for this study was the sea shelf of the Mikulinian (Eemian) Sea 115-130
312    ka ago. Marine sediments up to 50-70 m thick contained a large amount (up to 10%) of organic
313    residues of iodine-containing algae. Organic matter could enter sediments of the upper part of the
314    Vendian Formation during the diagenesis of marine precipitation [42].
315    *Retardation factor*
316    Retardation factor is determined by the formula [43, 6]:

317
$$R = 1 + M_s \cdot C_8^A / C_8^W \qquad (2)$$

318    where $M_w = \rho_m (1-n) / \rho_{water} n$ ; $C_8^A$ - solute concentration of $^{238}$U in the stationary solid,
319    μg/kg [44]; $C_8^W$ - measured concentration of $^{238}$U in solution at the point of sampling, μg/kg; $\rho_m$ -
320    mineral density, g/cm$^3$; $\rho_w$ - pore fluid density, 1 g/cm$^3$; $n$ - porosity.

321    For the study area, the following values of the parameters included in Eq. (2) were previously
322    obtained: $C_8^W$ = 5 µg/kg (from 23 definitions of uranium concentrations in fresh water in a Vendian
323    aquifer [28]; $n$ = 0.23 (from 52 determinations) and $\rho_m$ = 2.75 g/cm³ (from 52 determinations); $M_s$ =
324    9.2065 [27].
325    $C_8^A$ can be taken as the average value of U content in adsorbed elements of the red siltstones =
326    23 µg/kg (Table 3), because green siltstones occupy an insignificant volume in the deposits of the
327    Padun formation of the Vendian compared to red siltstones. However, this value characterizes the
328    entire volume of rock that was crushed before the experiments. Under natural conditions, the
329    movement of water in siltstones and sandstones occurs along pores and cracks, characterized by the
330    value of open porosity. From this open volume, uranium adsorption occurs, which determines the
331    value of the retardation factor. Therefore, as a first approximation, we can take:

332    $$R = 1 + M_s \cdot C_8^A / C_8^W \cdot n \qquad\qquad (3)$$

333    Calculations by the formula (3) give the value of the retardation factor 10.73.
334    In Malov [27], the average value of the ratio $R:p$ = 24 was determined for a Vendian aquifer,
335    where $p$ is the recoil loss factor. That is, at $R$ = 10.73, the value of $p$ will be 0.45.
336    The obtained values (10.73 and 0.45) apparently characterize the upper limits of $R$ and $p$,
337    repectively.

338    **6.    Conclusions**

339    The partial extraction procedure was used to reconstruct the redistribution processes of
340    uranium isotopes in certain mineral phases of the aquifer of sandy-clay deposits of the Vendian.
341    Red siltstones are depleted in uranium in relatively readily soluble mineral phases. The
342    concentration of adsorbed uranium was established as 15.8±2.1 - 30.5±3.9 µg/kg. This accounts for
343    0.35 - 1.6% of its total amount in rocks of this type. Carbonate minerals contain even less uranium:
344    7±1 – 19.8±2.5 µg/kg, i.e. 0.16 - 1%. In iron hydroxides and the most readily soluble aluminosilicates,
345    uranium concentrations are in the range 168±24 – 212±28 µg/kg. The most insoluble fraction contains
346    1.65±0.21 – 4.32±0.45 mg/kg of uranium. In green siltstones, the concentration of adsorbed uranium
347    is much higher: 106±14 - 364±43 µg/kg (0.56 - 4.37%). Carbonate minerals and amorphous iron oxides
348    contain 1.91±0.21 – 2.34±0.26 mg/kg of uranium. In aluminosilicates and a clay/quartz resistate,
349    uranium concentrations are 5.6±0.5 – 16.8±1.4 mg/kg. Such a distribution of uranium in various types
350    of rocks is consistent with the earlier assumption about the removal of uranium from red siltstones
351    in the last 0.9 Ma and its conservation in green siltstones.
352    Elevated values of $^{234}U:^{238}U$ activity ratio prevail in the adsorbed material and iron hydroxides.
353    In aluminosilicates and clay/quartz resistate, the values decrease. This indicates the replacement of
354    primary sedimentogenic uranium by secondary hydrogenic uranium adsorbed on the surface of
355    minerals and coprecipitated with iron hydroxides.
356    The results obtained made it possible to carry out preliminary quantitative estimates of the
357    retardation factor and recoil loss factor of uranium in the groundwater of siltstones of the Vendian
358    aquifer.
359    At the same time, some uncertainty in the interpretation of the high U contents and high
360    $^{234}U:^{238}U$ activity ratios in green siltstones obtained in this work should be noted. This requires
361    additional research on a more representative number of samples. Also, the relationship between the
362    extraction solutions and the mineral phases has not yet been precisely established. The mineral
363    phases that were dissolved during the sequential extraction procedure should be examined using
364    X-ray powder diffraction (XRD) analysis and scanning electron microscopy (SEM).

**Author Contributions:** Conceptualization, formal analysis, writing—original draft preparation, Alexander I. Malov; methodology and investigation, Sergey B. Zykov.

**Appendix A**

**Description of the thin sections of core samples**

Thin sections of core samples (n=5) were prepared in epoxy resin. Thin sections were examined under transmitted, polarized, and reflected light using optical microscopy to determine the minerals and the textural features of the rocks.

1.  *Green siltstones 66.7-66.8 m*

The sandy siltstone has a light greenish-gray color. The texture of the rock is heterogeneous, due to the chaotic arrangement of clastic grains and the presence of spots up to 0.4 mm in size with an iron-carbonate aggregate. Clastic material is 70-80% and is represented by grains of quartz, feldspar and quartzite rocks; the composition is dominated by quartz grains. Among feldspars where plagioclases and potassium feldspars are diagnosed, plagioclases prevail. The grain size varies from 0.02 to 0.15 mm; grains up to 0.2 mm in size are rarely found. The surface of the grains is corrosive. Single grains of accessory minerals are noted - tourmaline, ilmenite, epidote, zircon. On separate grains of quartz and feldspar, a regenerative rim is fixed. Some fragments of quartz and feldspar are sericitized. In the rock, single plates of colorless and colored mica up to 0.15-0.25 mm in size are diagnosed; this mica is diagenetic. Film-pore clay-ferruginous cement predominates, and cementation due to regeneration is also fixed. Marks, lenses (not exceeding 0.4-0.5 mm in size) with limonite-goethite and ferruginous-carbonate cement are noted. Carbonate is represented by calcite and it is formed later than limonite-goethite aggregate. Individual detrital grains are partially replaced by a ferruginous carbonate aggregate. Limonite-goethite and carbonate aggregates in cement are epigenetic. Most likely, compaction of sedimentary material, hydromica of cement in siltstone, and a high content of deformed plates are associated with dynamic changes. That is, the structural adjustment of cement is due to the influence of tectonic processes and hydrothermal solutions in the process of formation of kimberlite fields.

2.  *Red sandstones 75.2-75.3 m*

Sandstone oligomictic fine-grained silty has brown color with light streaks. Rounded spots 1.0–2.0 mm in size with carbonate cement are fixed in the rock; their location is subparallel. The slanting texture due to particle size distribution is not clearly expressed. In some areas, a random distribution of clastic material is noted. Clastic material is represented by grains of quartz, feldspar and quartzite rocks; the composition is dominated by quartz grains. The size of clastic grains varies from 0.03-0.04 mm to 0.2-0.25 mm. Grain rounding is mostly good and medium. The grain surface is corrosive; regenerative rim is fixed on separate fragments of quartz and feldspar. Separate fragments of quartz and feldspar are sericitized. There are single plates of green mica up to 0.12-0.15 mm in size, which fill individual pores and sometimes partially replace detrital grains. Most likely this mica is epigenetic. Film-pore clay-ferruginous cement predominates, and cementation due to regeneration is also fixed. Spots with limonite-goethite and ferruginous-carbonate cement are noted. Carbonate is represented by calcite and is formed later than limonite-goethite aggregate. Individual detrital grains are partially replaced by a ferruginous carbonate aggregate. Limonite-goethite and carbonate aggregates in cement are epigenetic.

3.  *Variegated siltstones 83.9-84 m*

Siltstone with indistinctly expressed oblique and banded textures. Striping does not coincide with layering; alternation of brown and gray, greenish-gray rocks does not form layers. Cross-bedding is due to the presence of argillite microlenses. The composition of this rock does not differ from the sandstones and siltstones that are described in the above.

4.  *Red siltstones    94-94.1 m*

Oligomictic siltstone of brown color with indistinctly expressed cross-layered texture. The oblique texture is due to a poorly defined granulometric sorting of clastic material and the presence

of argillite microlenses. Breccia is due to the presence of areas with a random distribution of clastic material, which is associated with sedimentation processes. The presence of sites with limonite-goethite cement is due to epigenetic processes. Clastic material, as in previous thin sections, is represented by grains of quartz, feldspar and quartzite rocks, quartz grains dominate in the composition. The size of clastic grains varies from 0.03-0.04 mm to 0.15-0.2 mm. Grain rounding is mostly average and good. The grain surface is corrosive; a regenerative rim is fixed on separate fragments of quartz and feldspar. Some fragments of quartz and feldspar are sericitized. Rare plates of colorless mica, which are diagenetic, are fixed in this strain. By the nature of the filling, the cement is not continuous, the number of hollow pores is insignificant. Film-pore clay-ferruginous cement predominates, and cementation due to regeneration is also fixed. Spots with limonite-goethite and ferruginous-carbonate cement are noted. Carbonate is represented by calcite and it is later than limonite-goethite aggregate. Limonite-goethite and carbonate aggregates in cement are epigenetic.

    5.   *Green siltstones 99.5-99.6 m*

        Oligomictic siltstone sandy with indistinctly expressed oblique and banded textures. The color of the strain is light greenish gray. In terms of composition and structural-textural features, siltstone does not differ from the rocks that are described in the above.

## References

1.   Chkir, N., Guendouz, A., Zouari, K., Hadj Ammar, F., Moulla, A.S.. Uranium isotopes in groundwater from the continental intercalaire aquifer in Algerian Tunisian Sahara (northern Africa). *J. Environ. Radioact*. **2009**, *100*, 649–656.

2.   Dhaoui, Z., Chkir, N., Zouari, K., Ammar, F.H., Agoune, A. Investigation of uranium geochemistry along groundwater flow path in the Continental Intercalaire aquifer (Southern Tunisia). *J. Environ. Radioact*. **2016**, *157*, 67–76.

3.   Priestley, S.C., Payne, T.E., Harrison, J.J., Post, V.E.A., Shand, P., Love, A.J., Wohling, D.L. Use of U-isotopes in exploring groundwater flow and inter-aquifer leakage in the south-western margin of the Great Artesian Basin and Arckaringa Basin, central Australia. *Appl.Geochem*. **2018**, *98*, 331–344.

4.   Suksi, J., Rasilainen, K., Marcos, N. U isotopic fractionation - a process characterising groundwater systems. In: Merkel, B.J., Hasche-Berger, A. (eds), *Uranium in the Environment*. Springer-Verlag: Berlin, Heidelberg, **2006**; pp. 683-690.

5.   Chabaux, F., Bourdon, B., Riotte, J. U-series geochemistry in weathering profiles, riverwaters and lakes. In: Krishnaswami, S., Cochran, J.K. (eds), *U/Th series radionuclides in aquatic systems*, vol 13, Radioactivity in the environment. Elsevier: New York, **2008**; pp. 49–104.

6.   Porcelli, D. Investigating groundwater processes using U- and Th-series nuclides. *Radioact. Environ.* **2008**, *13*, 105–153.

7.   Maher, K., DePaolo, D.J., Lin, J.C.F. Rates of silicate dissolution in deep-sea sediment: in situ measurement using U-234/U-238 of pore fluids. <u>*Geochim. Cosmochim. Acta*</u> **2004**, *68*, 4629-4648.

8.   Ivanovich, M., Fröhlich, K., Hendry, M.J. Uranium-series radio nuclides in fluids and solids, Milk River aquifer, Alberta, Canada. *Appl. Geochem*. **1991**, *6*, 405–418.

9.   Chabaux, F., Dequincey, O., Leveque, J.J., Leprun, J.C., Clauer, N., Riotte, J., Paquet, H. Tracing and dating recent chemical transfers in weathering profiles by trace-element geochemistry and U-238-U-234-Th-230 disequilibria: the example of the Kaya lateritic toposequence (Burkina-Faso). *CR Geosci* **2003**, *335*, 1219–1231.

10.  Dosseto, A., Bourdon, B., Turner, S. Uranium-series isotopes in river materials: Insights into the timescales of erosion and sediment transport. *Earth Planet Sci Lett* **2008**, *265*, 1–17.

11. Vigier, N., Bourdon, B. Chapter 27. Constraining Rates of Chemical and Physical Erosion Using U-Series Radionuclides. In: M. Baskaran (ed.), *Handbook of Environmental Isotope Geochemistry, Advances in Isotope Geochemistry*. Springer-Verlag: Berlin, Heidelberg, **2011**, pp. 553-571.

12. Duff, M.C., Coughlin, J.U., Hunter, D.B. Uranium co-precipitation with iron oxide minerals. *Geochim Cosmochim Acta* **2002**, *66*, 3533–3547.

13. Giammar, D.E., Hering, J.G. Timescale for sorption-desorption and surface precipitation of uranyl on goethite. *Environ Sci Technol* **2001**, 35, 3332–3337.

14. Singer, D.M., Maher, K., Brown, G.E. Jr. Uranyl-chlorite sorption/desorption: evaluation of different U(VI) sequestration processes. *Geochim Cosmochim Acta* **2009**, *73*, 5989–6007.

15. Tricca, A., Wasserburg, G. J., Porcelli, D., Baskaran, M. The transport of U- and Th-series nuclides in a sandy unconfined aquifer. *Geochim. Cosmochim. Acta* **2001**, *65*, 1187–1210.

16. Lowson, R.T., Short, S.A., Davey, B.G., Gray, D.J. $^{234}$U/$^{238}$U and $^{230}$Th/$^{234}$U activity ratios in mineral phases of a lateritic weathered zone. *Geochim. Cosmochim. Acta* **1986**, *50*, 1697–1702.

17. Payne, T.E., Edis, R., Fenton, B.R., Waite, T.D. Comparison of laboratory uranium sorption data with 'in situ distribution coefficients' at the Koongarra uranium deposit, Northern Australia. *J. Environ. Radioact.* **2001**, *57*, 35–55.

18. Dabous, A.A., Osmond, J.K., Dawood, Y.H. Uranium/thorium isotope evidence for groundwater history in the Eastern Desert of Egypt. *J. Arid Environ.* **2002**, *50*, 343–357.

19. Yanase, N., Nightingale, T., Payne, T., Duerden, P. Uranium distribution in mineral phases of rock by sequential extraction procedure. *Radiochim. Acta* **1991**, *52-53*, 387-393.

20. Malov, A.I. Evolution of the uranium isotopic compositions of the groundwater and rock in the sandy-clayey aquifer. *Water (Switzerland)* **2017**, *9* (12), 910.

21. DePaolo, D.J., Maher, K., Christensen, J.N., McManus, J.,. Sediment transport time measured with U-series isotopes: Results from ODP North Atlantic drift site 984. *Earth Planet Sci Lett* **2006**, *248*, 394–410.

22. Maher, K., DePaolo, D.J., Christensen, J.N. U-Sr isotopic speedometer: fluid flow and chemical weathering rates in aquifers. *Geochim Cosmochim Acta* **2006**, *70*, 4417–4435.

23. Tessier, A., Campbell, P.G.C., Bisson, M. Sequential extraction procedure for the speciation of particulate trace metals. *Anal. Chem.* **1979**, *51*, 848–851.

24. Hall, G.E.M., Vaive, J.E., Beer, R., Hoashi, M. Selective leaches revisited, with emphasis on the amorphous Fe oxyhydroxide phase extraction. *J. Geochem. Explor*. **1996**, *56*, 59–78.

25. Quevauviller Ph., Rauret, G., López-Sánchez, J.-F., Rubio, R., Ure, A., Muntau, H. Certification of trace metal extractable contents in a sediment reference material (CRM601) following a three-step sequential extraction procedure. *Sci. Total Environ.* **1997**, *205*, 223–234.

26. Sutherland, R.A., Tack, F.M.G., Tolosa, C.A., Verloo, M.G. Metal Extraction from Road Sediment using Different Strength Reagents: Impact on Anthropogenic Contaminant Signals. *Environ Monit Assess* **2001**, *71-3*, 221-242. https://doi.org/10.1023/A:1011810319015

27. Malov, A.I. Estimation of uranium migration parameters in sandstone aquifers. *J. Environ. Radioact.* **2016**, *153*, 61-67.

28. Malov, A.I. Evolution of the groundwater chemistry in the coastal aquifers of the south-eastern White Sea area (NW Russia) using $^{14}$C and $^{234}$U-$^{238}$U dating. *Sci. Total Environ.* **2018**, *616–617*, 1208-1223.

29. Andreas, J.N., and Kay, R.L.F. The evolution of enhanced $^{234}$U/$^{238}$U activity ratios for dissolved uranium and groundwater dating. 4th Int. Conf. on Geochronology, Cosmochronology and Isotope Geology, Denver, Colo., 1978. *U.S. Geol. Surv., Open-File Rep*. **1978**, 78-701, 11-13.

30. Fröhlich, K., and Gellermann, R. On the potential use of uranium isotopes for groundwater dating. *Chem. Geol*. **1987**, *65*, 67-77.

31. Andreas, J.N., and Kay, R.L.F. The U contentand[234]U/[238]U activity ratios of dissolved uranium in groundwaters from Triassic sandstones in England. *Isotope Geoscience* **1983**, *1*, 101- 117.

32. Stankovsky, A.F., Verichev, E.M., Grib, V.P., et al. The Vendian in the Southeastern White Sea Region. *Izv. Akad. Nauk SSSR, Ser. Geol.* **1981**, *2*, 78–87.

33. Stankovsky, A.F., Verichev, E.M., Dobeiko, I.P. The Vendian in Southeastern White Sea Region. In: *The Vendian: Historical-Geological and Paleontological Evidence*, vol. 2: Stratigraphy and Geological Processes. Nauka: Moscow, **1985**, 67–76 (in Russian).

34. Malov, A.I. Water-Rock Interaction in Vendian Sandy-Clayey Rocks of the Mezen Syneclise. *Lithol. Miner. Resour.* **2004**, *39-4*, 345–356.

35. Grazhdankin, D.V., Podkovyrov, V.N., Maslov, A.V. Paleoclimatic Environments of the Formation of Upper Vendian Rocks on the Belomorian-Kuloi Plateau, Southeastern White Sea Region. *Lithol Miner Resour* **2005**, *40*, 232. https://doi.org/10.1007/s10987-005-0024-x

36. Bonotto, D.M., Andrews, J.N. The mechanism of [234]U/[238]U activity ratio enhancement in karstic limestone groundwater. *Chem. Geol. (Isot. Geosci. Sec.)* **1993**, *103*, 193-206.

37. Bonotto, D.M., Andrews, J.N. The transfer of uranium isotopes [234]U and [238]U to the waters interacting with carbonates from Mendip Hills area (England). *Appl. Radiat. Isotopes* **2000**, *52*, 965-983.

38. Singh, S. P., Tack, F. M. G., Verloo, M. G. Solid-phase distribution of heavy metals as affected by single reagent extraction in dredged sediment derived surface soils. *Chem. Spec. Bioavail*. **1996**, *8*, 37–43.

39. Malyshev, V.I., Bakhur, A.E., Manuylova, L.I. et a. *Methods for measuring the volumetric activity of uranium isotopes (234, 238) in natural water sample alpha spectrometry with radiochemical separation*. VIMS: Moscow, **1999a** (in Russian).

40. Fröhlich, K. Dating of old groundwater using uranium isotopes – principles and applications. In: *Isotope methods for dating old groundwater.* IAEA: Vienna, **2013**, 153-178.

41. Malyshev, V.I., Bakhur, A.E., Manuylova, L.I. et al. Methods for measuring the specific activity of uranium isotopes (234, 238) in soils, sediments, rocks and building materials alpha spectrometry with radiochemical separation. VIMS: Moscow, **1999b** (in Russian).

42. Malov, A.I. Application of Geological Benchmarks for Determining Groundwater Residence Time in the Aquifer Based on Uranium Isotope Data: Evidence from the Severnaya Dvina Basin. *Lithol. Miner. Resour*. **2013**, *48-3*, 254–265.

43. Krishnaswami, S., Graustein, W. C., Turekian, K. K., and Dowd, J. F. Radium, thorium and radioactive lead isotopes in groundwaters: Application to the in situ determination of adsorption-desorption rate constants and retardation factors. *Water Resources Res*. **1982**, *18*, 1663-1675.

44. Pearson, F.J., Norowha, C.J., Andrews, R.W. Mathematical modelling of the distribution of natural ^{14}C, [234]U, and [238]U in a regional groundwater system, *Radiocarbon* **1983**, *25*, 291–300.